Aerosol and Air Quality Research, 14: 806–817, 2014

ISSN: 1680-8584 print / 2071-1409 online
doi: 10.4209/aaqr.2013.02.0062

Aerosol Optical Properties and Composition over a Table Top Complex Mining Area in a Monsoon Trough Region

R. Latha[1*], B.S. Murthy[1], Manoj Kumar[2], S. Jyotsna[2], K. Lipi[2], G. Pandithurai[1], N.C. Mahanti[2]

[1] *Indian Institute of Tropical Meteorology, Dr. Homi Bhabha Road, Pashan, Pune – 411008, India*
[2] *Centre of Excellence in Climatology, Birla Institute of Technology, Mesra, Ranchi – 835215, India*

ABSTRACT

Aerosol physiochemical properties over a varied mining plateau region at the eastern end of a monsoon trough are reported for the first time and analyzed at different time scales. Aerosol optical depth (single scattering albedo, SSA) is found to be 0.49 (0.9) in pre-monsoon, 0.4 (0.94) in monsoon, 0.46 (0.92) in post-monsoon, and 0.36 (0.89) in winter, with an annual mean of 0.43 (0.91). The volume-size distribution is tri-modal, with 0.02 (ultra-fine), 0.2 (accumulation) and 7 (coarse) μm, but with seasonal signatures. The angstrom exponent (AE) varies along with the AOD, especially in winter, although they are inversely related to each other during monsoons; the increase in size may be due to the effect of humidity. AOD_{bc} varies between 13.4%–4.7% of the total aerosols, with the highest contribution in March, when forest burning in the north east is at its peak. BC is the lowest in July, the mid monsoon month with the minimum biomass burning and brick-kiln activities. It is likely that the interactions of various minerals and intermittent rains help keep the aerosol size in a mixed state with regard to the relation between AE and AOD, although more work is needed to confirm this. The chemical composition of aerosols is derived from an aerosol chemical model based on the measured amount of black carbon and the assumed components. These components are selected based on back trajectories and earlier reports from the region. Their concentrations are adjusted by constraining the model output AOD and SSA to match (±2% @ 500 nm) that observed by a sun-sky radiometer. The chemical compositions of the winter and post-monsoon months are similar, while pre-monsoon period has more coarse mode minerals, and the monsoon period has more sea-salt (accu.). The component mass concentrations were grouped into various size bins based on their modal radii, and the results indicate that PM_1 is at its maximum in winter whereas $PM_{2.5}$ is highest in the post-monsoon period. Monsoons leads to the effective washout of 2.5–10 μm sized particles.

Keywords: Aerosol optics; Particulate matter; Mineral transport; Mixed mining region; Chemical model.

INTRODUCTION

Aerosols are studied through various considerations such as optical properties in terms of visibility (e.g., Silvia, 2002) or radiative forcing (e.g., Haywood and Ramaswamy, 2012); mass concentration for health related pollution (e.g., Dockery and Pope III, 1994). They are also studied for chemical properties in view of deposition and wash-out causing acid rain (e.g., Scudlark and Church, 1988) and cloud condensation nuclei connected to precipitation (e.g., Novokov and Penner, 1993). Aerosol size distribution modifies the cloud droplet size distribution spectra (e.g., Bréon *et al.*, 2002). The radiative forcing by aerosols modulates surface fluxes (Ramanathan *et al.*, 2001) hence also interferes with agricultural production (Stanhill and Cohen, 2001).

Indo Gangetic Basin (IGB) in India is highly important for Indian agricultural economy as it has got majority of cultivable land and it is also geographically important as it is almost at the foothills of Himalayas. The dust that is transported from Arabian and Thar deserts through IGB to the west and Bay of Bengal in the east gets mixed with industrial/black carbon aerosols on the way, as there are moderately high plateaus to the south of IGB (e.g., Srivastava *et al.*, 2012). Many stations over IGB are covered under AErosol RObotic NETwork (AERONET) or Indian Space Research Organization (ISRO) Aerosol Radiative Forcing over India (ARFI), ISRO-ARFI network (Moorthy *et al.*, 2011) but in this study we prefer to consider stations like Kanpur, Gandhi College (Balia), Darjeeling, located around Ranchi for comparison of their aerosol properties (e.g., Singh *et al.*, 2004; Chatterjee *et al.*, 2010, 2012; Srivastava *et al.*, 2012). While a reduction in aerosol optical depth (AOD) is observed from west to east of IGB as reported by Srivastava *et al.* (2012) in general and in particular during

* Corresponding author.
Tel.: 91-20-25904348; Fax: 91-20-25865142
E-mail address: latha@tropmet.res.in

pre-monsoon period, northern hilly regions viz. Nainital, Dibrugarh, Darjeeling experience a high AOD during pre-monsoon period due to dust transported from Arabian deserts (Dumka *et al.*, 2008; Chtatterjee *et al.*, 2010; Gogoi *et al.*, 2011). Kumar *et al.* (2011) report an increase in ozone, BC concentration and AOD (at 500 nm) by 34%, 145% and 150% respectively in the central Himalayas due to burning of agricultural residue in the pre-monsoon months. Further, their trajectory analyses show a deceleration of wind flow during the fire-impacted period indicating convection that helps transfer of aerosols present to higher levels. In contrast to other stations in IGB, the hill station, Darjeeling (Chatterjee *et al.*, 2010, 2012) indicates an abundance of fine particles (~162% of annual mean) through pre-monsoon period as well, though variation in AOD is largely similar. Chemical composition and particulate matter analysis of Decesari *et al.* (2010) indicate that considerable PM_{10} aerosols are transported to their high altitude aerosol observatory in Nepal all the yearlong from foothills of Himalayas through up-valley flows. It is interesting to note that coarse mode PM_{10} aerosols are transported even in the significantly stable winter time as well. Wang *et al.* (2009) discussed anthropogenic absorbing aerosols as the cause of Indian summer monsoon's northward shift especially during the onset of season; in this context knowledge of trough region aerosol characteristics gains more importance since the summer monsoon is deterministic in India's economy and agricultural yield.

The current station under study Ranchi (85.3°E, 23.5°N, 650 m MSL) is situated at the south east end of IGB but is a plateau area, does not have any significant representation in terms of aerosol characterization. It is also a varied mining region (Fig. 1) implying that aerosols present there can be expected to have quite unique physical and chemical properties and mixing states. Table top mining related particulate pollution is an increasing concern as biological experiments by Knuckles *et al.* (2013) show that even 24 hours exposure caused considerable micro-vascular dysfunction and the strong valley flows from plateau easily transport pollutants downhill than uphill. Hence constraining and finding abatement measures on the plateau pollution is essential to save further degradation of adjacent valleys. Thus knowledge of the aerosol characteristics is essential as other lower altitude regions around also fall in the heavy mining belt of India where abatement measures are a concern since long (Ghose and Majee, 2001; Ghose, 2007). The wind reversals happening through 360° at this station also support existence of distinctive aerosol nature.

Through the current study we present the monthly and seasonal variation of aerosol optical and chemical properties including volume size distribution over the Ranchi plateau. Chemical composition of aerosols is derived from aerosol optical model by using measured black carbon mass concentration with other possible components adjusted so that the model derived AOD and SSA match with those obtained from sun-sky radiometer. An attempt is also made to inspect whether all the absorption is caused by BC alone or a mixture of BC or any other possible absorbing aerosols.

LOCATION DETAILS, EXPERIMENTAL SETUP AND CONCURRENT OTHER MEASUREMENTS

Fig. 1 presents a mineral map of India with Ranchi marked specifically to show the diversity in minerals and its plentiful availability. It has mines of coal and bauxite to the west; coal, asbestos and graphite to the north; iron, manganese, asbestos, coal and chromites to the east and iron, gypsum, copper, manganese and coal to the south.

The skyradiometer, model POM1-L (PREDE Inc, Japan make) that measures sky radiances directly and that of aureole to derive aerosol properties through inversion algorithm, SKYRAD.pack (used in SKYNET aerosol-radiation network; http://atmos.cr.chiba-u.ac.jp/aerosol/skynet), is used to make measurements of aerosols during daytime under clear sky conditions. Aoki and Fujiyoshi (2003) provide a detailed technical description of skyradiometer function. It measures both direct solar irradiance (every 1 min) and diffuse sky radiation at either 10 min time interval or 0.25 step in air mass at 7 wavelengths (0.315, 0.4, 0.5, 0.675, 0.87, 0.94, 1.02 μm); we opted 10 min interval for this study. Calibration methodology and data reduction procedures or quality checks for this instrument are followed as per Nakajima *et al.* (1996) and Boi *et al.* (1999).

The sky radiometer is installed on the terrace of Department of Applied Mathematics building at BIT-Ranchi (23.5°N, 85.3°E, 600 m AMSL) taking care to avoid as much obstructions around as possible in the scanning pathway as BIT campus is thickly populated with tall Salwood trees and it was not permitted even to crop the branches of trees. Owing to the latitude (23.5°N) of the station, sky-radiometer did the vertical plane scan only during summer and some of the late evening data was lost due to presence of a tall tree to the west; being an eastern location, sunrise and sunset are always early with respect to local time.

Backward trajectories of wind (Figs. 2(a), (b) and (c)) for 5 days for 2nd week of every month are obtained through NOAA- Hysplit trajectory model (Draxler and Rolph, 2013) using GDAS data for surface, 1500 m and 3500 m altitudes and mixed layer depth (used in OPAC) is obtained from Giovanni (disc.sci.gsfc.nasa.gov/giovanni#maincontent) MERRA (Acker and Leptoukh, 2007). The meteorological observatory (LATAMOS) maintained by Birla Institute of Technology, Ranchi consists of a 32 meter tower mounted with meteorological sensors at different levels, another small post mounted with radiation (Table 1) sensors. Incoming solar radiation in short wave band of 0.3–3.0 μm, $SW_{in,}$ is collected at 1Hz and averaged for 1min and logged. Apart from tower, it also has a conventional observatory (WMO/ IMD standards) with surface based meteorological sensors (Vaisala make) such as pan evaporimeter, sunshine hour recorder etc. Data from conventional observatory viz. wind, humidity, temperature, rainfall (Fig. 3(a)) provides meteorological background. Monthly-mean wind speed increases from winter to pre-monsoon, highest (3 m/s) in June before the onset of rains. Winds are relatively high and consistent in pre-monsoon period while they remain high in monsoon with lower wind maxima, revealing the influence of large scale flow. While humidity reduces steadily during

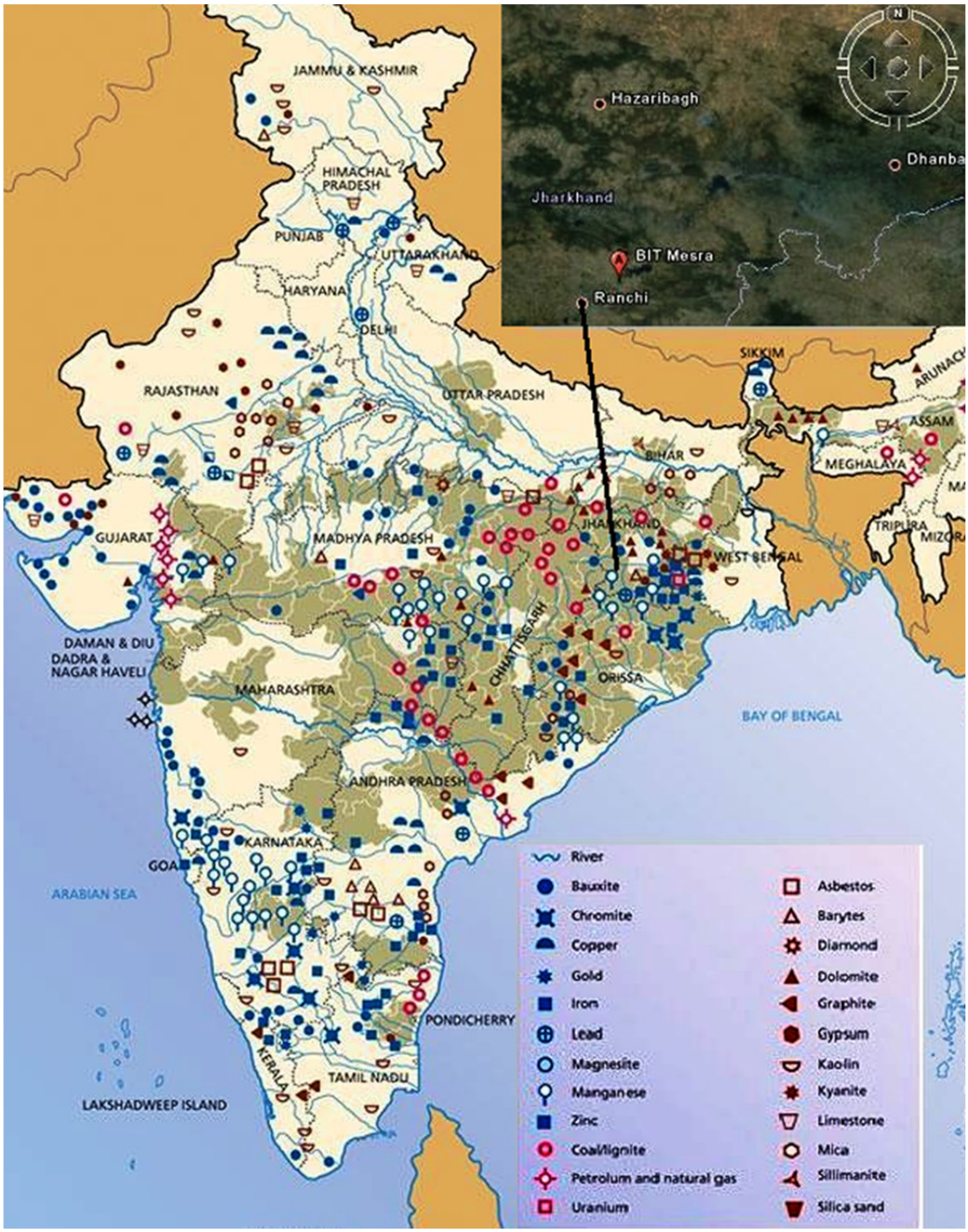

Fig. 1. Mineralogical map of India (source: Centre for Science and Environment, New Delhi) with the observation station, Ranchi shown in inset as Google map.

pre-monsoon till March, thundershowers enhance it during April–June whereas post monsoon and winter continues to have better humidity levels and highly variable rainfall. After 2 months of almost no rainfall, January 2011 had a fair amount of rainfall.

SKYRADIOMETER DATA SCREENING AND METHODOLOGY

Aerosol optical properties are obtained by inverting the sun-sky radiances using the inversion algorithm viz. SKYRAD.pack version 4.2 (Table 1). Collected raw data are processed first to obtain calibration constant on monthly basis, checked for least deviation with the previous month and the calibration constant thus obtained is used for second level processing. The SKYRAD.pack uses less than 0.02 convergence error to obtain calibration constant through

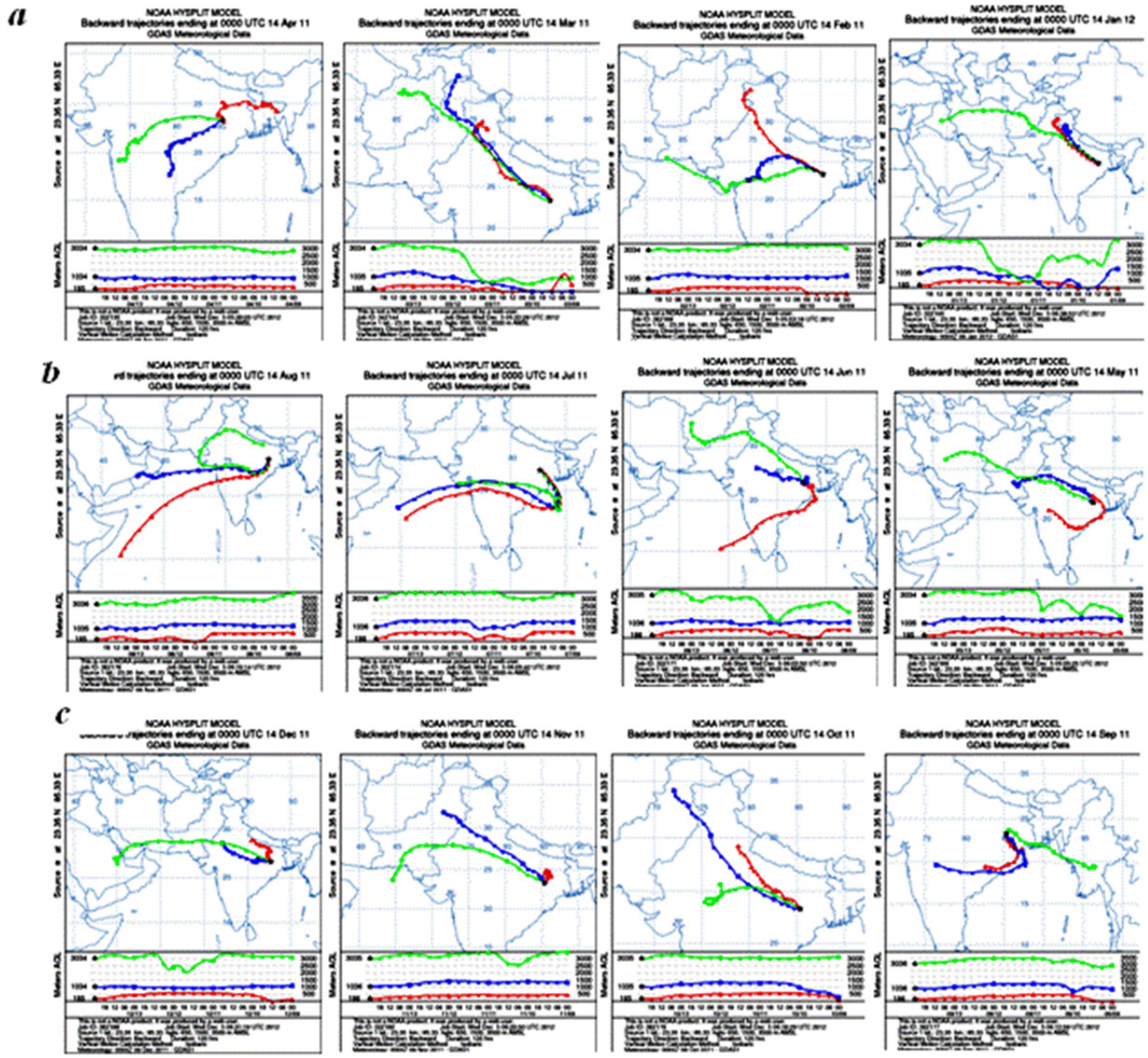

Fig. 2. a) 7 day back trajectories derived from NOAA-Hysplit back trajectory analysis based on 14th of every month at the location: January–April, 2011(right to left); b) Same as in Fig. 2(a) but for May–August; c) Same as in Fig. 2(a) but for September–December.

Table 1. Details of aerosol and other parameter sources/instruments/model/software used.

Parameter	Source/Instrument/reference/software
AOD, SSA, Angstrom exponent, Asymmetry parameter	Skyradiometer (PM-01-L, Prede) (315, 400, 500, 675, 870, 940, 1020 nm wavelengths)
Skyradiometer data analysis software	Skyradpack 4.2/5.0 (Nakajima *et al.*, 1996, organized by M. Yamano)
Down-welling Global Shortwave flux [0.3–3.0 μm]	Net Radiometer @1Hz averaged to 1 min Kipp & Zonen Model [CNR4]
BC and OC mass concentration	Aethalometer (AE-42, Magee Scientific *www.mageesci.com*)
BC-AOD, SSA, Angstrom, Asymmetry	OPAC (Hess *et al.*, 2002)
Mixed layer depth for OPAC	Giovanni-Monthly chemistry forcing data-PBL height (lat 1.25° × lon 1°)

improved Langley method and is capable of screening out the cloud contaminated data to a great extent. Further quality control is done by screening out the data that is above one standard deviation of daily mean for stringent cloud screening. Since the observation station has a tendency to get partly cloudy on most of the days of the year, we checked AOD

data for cloud affected hours, verified with the pyranometer data and decided to filter out all AOD data above 1.0 (due to clouds) to avoid any cloud contamination as a further quality check. Solid view angles are checked periodically on clear days but settings are not changed as the results showed little deviation from the initial installation values; however a limited offset tuning together with cleaning of lens are done once a week. Concurrent to AOD, other parameters viz. single scattering albedo (SSA), refractive indices (RI) real and imaginary and volume-size distribution are also obtained.

Black carbon (BC) concentration is also measured at the site during Jan-Dec 2011 using seven-channel aethalometer (model AE-47, Magee Scientific Company, USA; Table 1) in which BC mass concentration is obtained through 880 nm optical measurements. Operational and other details are available in the web page, http://www.mageesci.com/Aethalometer_book_2009.pdf. Data for September and December are not available due to instrumental problem and data for August is not used as there are only a few clear sky days and not statistically significant.

The chemical model OPAC (Optical Properties of Aerosols and Clouds; Hess *et al.*, 1988) allows different types of chemical components with different number concentrations as input that can be adjusted to match with the observed AOD and SSA @ 500 nm. In the present study, we have used suitable combination of components based on back trajectories and possible potential sources for different seasons (Table 2). Observed mixed layer height and humidity are used in OPAC with possible 4 chemical components other than measured BC. Number concentrations of components are fine tuned constraining the total number concentration to approximate the 'Urban' type in OPAC. The model output consists of number, mass, volume concentrations and mixing ratios of different components. As described in Sreekanth *et al.* (2007), AOD_{bc} is derived using OPAC by neglecting all other components but with only BC input. The volume-size distribution obtained from sky-radiometer observations is qualitatively verified with the volume concentration of OPAC components plotted against the modal-volume radii of respective components. Further sky-radiometer derived volume size distribution is converted to number size distribution to know approximate total number of PM_1, $PM_{2.5}$ and PM_{10} and compared the same with the mass concentration derived through OPAC in different bin sizes.

RESULTS AND DISCUSSION

Monthly and Seasonal Variations of Optical and Physical Properties

Fig. 3(b) shows variations of monthly-mean AOD, SSA, and refractive index real (RIR) and imaginary (RII) for 500 nm wavelength; while RIR indicates the classification of the material, RII relates to absorbing properties. AOD varies similar to RIR while SSA has similar trend like RII (Fig. 3(b)). Monthly mean AOD (indicated as stars) retrieved from MODIS-Terra is shown in Fig. 3(b) for comparison of satellite data with in-situ AOD. Evidently they match best when cloud cover is the least and when the atmosphere has an abundance of coarse mode aerosols (April–June).

Aerosols can be identified or grouped based on their refractive indices (Levoni *et al.*, 1997). Inferring the aerosol types on the basis of their refractive indices based on their work suggest an abundance of water soluble aerosols mixed with soot (SSA < 0.85; high absorption) in February–March changing to more dust-like (SSA > 0.9; more scattering) but mixed with soot in pre (April–May) and post monsoon (October–December). RIR also indicate that aerosols prevailing in both pre and post monsoon also exhibit some

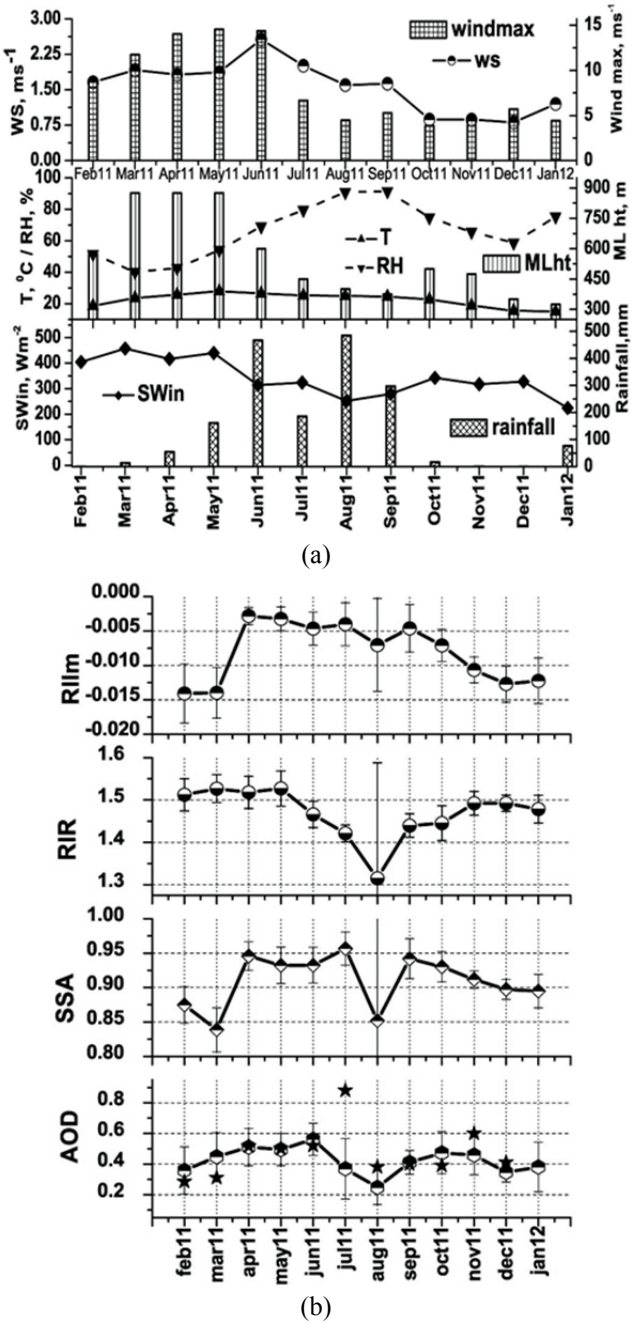

Fig. 3. a) Back ground meteorological parameters; wind speed, wind maximum, temperature, humidity, shortwave incoming radiation and rainfall for the year 2011; b) Monthly variation aerosol properties; AOD, SSA, RIR and RII. AOD from MODIS indicated by '*'.

Table 2. OPAC components assumed with details.

component	r_{mod}, V, μm	possible constituents
soot	0.018	black carbon (BC/EC) with density 1 g/cm^3
waso	0.029	sulphates and nitrates of Na, K, NH_4 and some part of OC
inso	6.0	soil particles with insoluble part of OC
minm	0.27	non-hygroscopic sub-micron mineral dust produced locally or transported
miam	1.6	---do----; but with higher radius
micm	11	---do---; but biggest size possible
ssam	0.94	sea salt particles than can get transported to part of inland during high winds with sea origin

influence of marine aerosol component. Similarly, monsoon period has a definite excess of marine component (sea salt) but it is mixed with some absorbing component, as indicated by SSA close to 0.9 is lower than sea salt aerosols those are highly scattering. This component is apparently other than soot, since observed BC is the least in these months. Source location and trajectories of parcels (Figs. 2(b) and 2(c)) conform to the properties of aerosols present at various times. They also point towards a possible influx of hematite from the iron ore mines to the south of the station with the wind blowing from south.

In March 2011 at Ranchi the aerosols exhibit an anomalous absorbing nature with the lowest SSA (0.84), though we see only a slight change in the RIR and almost no change RII. As per the detailed analysis and data set of fire counts/ sources by Venkataraman *et al.* (2006) March is the peak period of forest fire for NE India as well as central India. The wind trajectory fluctuates between northwest to north east during this month and it is capable of bringing in soot to higher levels in the atmosphere. Local emission around the month-end is also high with the festival "Holi" when large scale waste wood is burnt during "Holika Dahan/Dhuli Vandan".

Though the trajectory plots (Figs. 2(a) and 2(b)) at the ground level show change of direction in April (NE), May (S) and June (SE), under the prevailing well mixed conditions, dust from Thar region that gets transported to upper layers of atmospheres over Ranchi is capable of maintaining the coarse mineral dust influx apart from the dust raised by local winds. In pre-monsoon month April, volume size distribution (Fig. 4(a)) indicates highest peak close to but less than 10 μm supports the transport of dust from W-NW direction. Change in surface wind direction and pre-monsoon showers reduce coarse particle concentration in May hence its coarse volume stays below that of April. In June coarse mode volume exhibits a double step at 1–6 μm and at around 11 μm, shows the effect of both coarse dust particles and humidity. The first half of June often experiences dusty winds and in the later half it changes over to rains as evidenced by the observer records and rainfall data. Growth of aerosols due to humidity impact (Tang, 1996) is also a deciding factor of the scattering property in this period as the peak in the monthly volume size distribution beyond 10 μm (Fig. 4(a)) seems to be an outcome related to high humidity.

During monsoon period sea salt influx seems to help sustain the high coarse mode distribution as explained by Chatterjee *et al.* (2010) in their chemical analysis of aerosol data at Darjeeling, a hill station further north to Ranchi. At

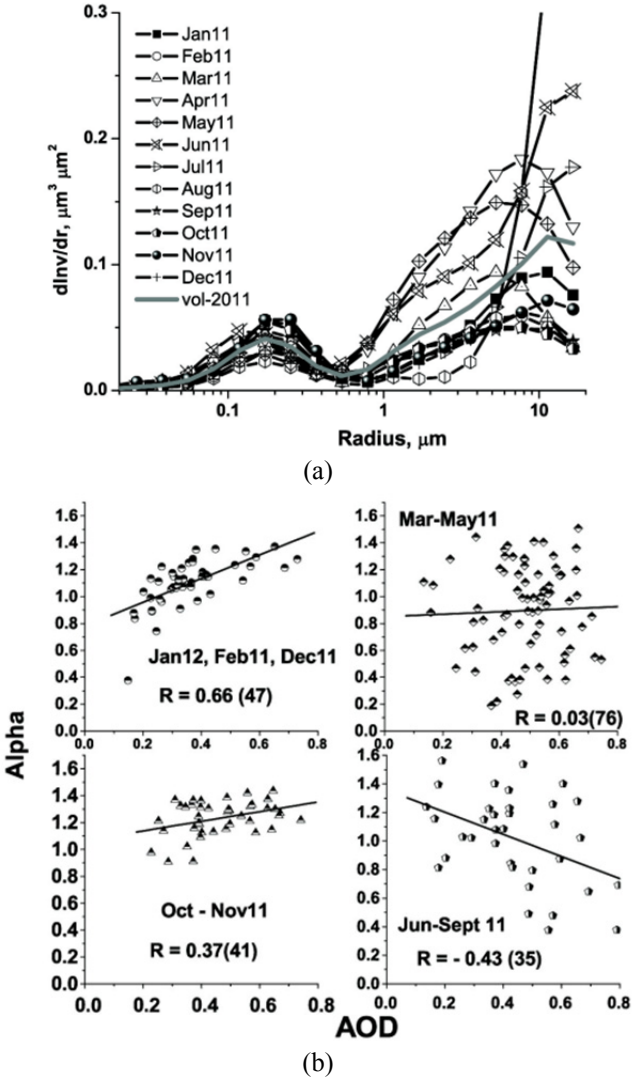

Fig. 4. a) Monthly volume-size distribution; b) AE vs. AOD on seasonal scale; dots represent individual day average, correlation coefficient (number of days) are included.

Ranchi aerosols have the least optical extinction (AOD) in August apparently due to wash out. Though the aerosol concentration reduces (minimum AOD) presence of absorbing particles restricts SSA to low values. We are cautious to state that as the data length is particularly small in August to rely on. The accumulation mode peak is the maximum in October–November that is caused by various activities around that time. Minute inspections of these

monthly volume-size distribution curves show a tri-modal distribution with a small peak in the nucleation mode particles in these months (Fig. 4(a); further illustrated in Fig. 5(b)). Burning activity that starts with Ramnavami in October to festival of lights, Deepawali in November, lots of crackers are burst that increases chemical/soot loading in the atmosphere. It is so significant that there are special studies conducted on aerosol loading in this period (e.g., Babu and Moorthy, 2001). Use of coal or firewood for warmers in winter further increases the soot aerosol loading of the atmosphere.

Angstrom Exponent, AE or α is the term indicating spectral dependency of AOD or aerosol size-AOD relations. α is calculated by the relation, $\alpha = -\ln(\tau1/\tau2)/\ln(\lambda1/\lambda2)$, where τ1 and τ2 are AODs at wave lengths λ1 and λ2 respectively. A best fit slope is obtained to find the AE between 400–1020 nm. Fig. 4(b) shows AE - AOD relation for different months with AE calculated for the entire wavelength range. Lee *et al.* (2010) proposed a classification of aerosol types depending on SSA and fine mode fraction and a class as "mixture" was suggested for aerosols having intermediate properties. The aerosols at Ranchi also may well be classified as "mixture" based on their AE-AOD variations and SSA values as the current results do not show demarcation of size based on AE values. The AE - AOD correlation coefficient falling below 0.6 (except for winter, 0.66) indicates uncertainty of dominant size (Fig. 4(b)). Thus it could be said that from December to February, increase in AOD is mainly caused by fine aerosols. In the dust dominated regions and during dust storms (Dey *et al.*, 2004; Moorthy *et al.*, 2007) AE vs. AOD show a clear, high negative correlation as coarse particles contribute to the increase in AOD. In Fig. 4(b) negative correlation is observed only during June–September In spite of the volume-size distribution (Fig. 4(a)) indicating the second peak (radius > 0.5 μm) much higher than the first peak (radius < 0.5 μm) in pre-monsoon as well as in monsoon months, an inverse relation between AE and AOD is absent in pre-monsoon. This behavior confirms that the aerosols fall into the category "mixture" (neither fine/absorbing nor coarse/scattering). Seasonal correlation of AE - AOD, shown in Fig. 4(b), is drastically low (0.03) in pre-monsoon season (March–May) having the highest data base of 76 days, proving the non-local and varied sources of aerosols while the same for winter (December, January, February) with a value of 0.66 indicates the dominant control of local sources which is corroborated by prevailing low wind speed.

Monthly averages are used to derive seasonal and annual optical properties (Fig. 5). Comparatively low AODs (–15% of annual mean) in winter associated with strongly absorbing (SSA is –4% of annual mean) nature changing over to larger AODs (+13% of annual mean) in pre-monsoon with higher scattering (SSA is –1% of annual mean), suggests that winter is characterized by relatively higher concentration of fine soot particles and reduced mixing height that gradually turns to increased influx of coarse dust particle along with higher mixing height in pre-monsoon which is consistent with the reports of other stations in the IGB north east (Chatterjee *et al.*, 2012) and north west (e.g., Singh *et al.*, 2004). Wind trajectories are also nearly similar. However,

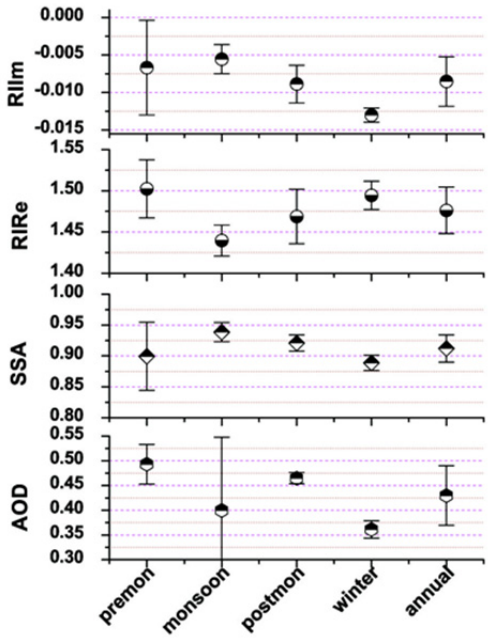

Fig. 5. Seasonal variation and annual mean of optical parameters.

during monsoon and post monsoon months the generalization of trends in IGB ceases; while some stations like Kanpur to the west (Singh *et al.*, 2004); monsoons are optically thick with high AOD. Darjeeling, located at the east (Chatterjee *et al.*, 2012) experiences thinnest aerosol layer in monsoon but for Dibrugarh, a station further to the north-east, post monsoon reports to be of minimum AOD (Gogoi *et al.*, 2011). AOD has an annual average of 0.43 that falls between AOD for monsoon (0.4) with the high standard deviation (SD) and AOD for post monsoon (0.46) with low SD. However, the highest AOD occurs in pre-monsoon (0.49). Unlike at Dibrugargh or Gandhi College (Gogoi *et al.*, 2011; Srivastava *et al.*, 2012) or Darjeeling (Chatterjee *et al.*, 2012) winter is optically thinnest (lowest AOD) at Ranchi for 2011. Rain-out in monsoon season certainly reduces aerosol concentration but high humidity aids the growth of aerosols and makes it more scattering irrespective of chemical composition thus resulting in enhanced AOD as well as SSA (Tang, 1996). The results show that SSA decreases seasonally from monsoon to winter thereafter increases a little during pre-monsoon. RII exactly follows SSA variations while RIR variation is opposite to that of SSA. Winter aerosols here are the most absorbing, and maintains the same nature throughout the season as indicated by minimum standard deviation (Fig. 5) reiterating the local signature.

Volume and Number Size Distribution

Seasonal variation of volume-size distribution further explains the behavior of AOD with the highest AOD corresponding to maximum area under the curve and the lowest corresponding to minimum area. Seasonal variation of number and volume size distributions are shown in Fig. 6. Number (Fig. 6(b)) and volume (Fig. 6(a)) size distributions indicate three peaks corresponding to radii of 0.02 μm, 0.2

μm and 7 μm representing ultra fine, fine and coarse modes respectively. The 3 modes are shown individually with dashed curves. The results are to be carefully interpreted as Nakajima (1996) estimated the error in volume-size distribution as 20% for the middle range and 35–100% at the edges. Yang and Wenig (2009) suggested that if the volume in the coarse (> 7 mm) or ultrafine (< 0.03 mm) exceeded the mean value of the whole spectrum, then they needed to be considered as anomaly and is to be discarded as they could be an outcome of cloud effect. However, in our case ultrafine range does not show such anomaly any time but the coarse mode is very high in June–August (Fig. 4(b)). Though they are considered, it results only in limited errors. A noticeable feature of this station (Fig. 6(a)) is that peak radii in fine and coarse modes for pre-monsoon are less than that for monsoon and post-monsoon but the area under the curve for pre-monsoon is much higher in comparison. In pre-monsoon, coarse mode volume concentration dominates as compared to other seasons and is attributable to transport of mineral dust from IGB and north east regions as indicated by back trajectories (Figs. 2(a) and (b)). The increase in fine and ultrafine mode (peak radii 0.2 μm and 0.02 μm respectively) during post monsoon illustrates wind assisted fine dust loading of atmosphere after the rains. Increase of fine BC and ash due to re-start of biomass burning and other activities adds to it. Winter is the least in volume concentration for both fine and coarse modes. Number concentration is derived from volume concentration by dividing it by $4/3\pi r^3$. They maintain an almost inverse relation as the aerosols in the ultrafine mode having maximum number contribute to the minimal volume and vice versa in the coarse mode; for the same reason peak radii corresponding to peaks in number concentration are less than those for volume concentration.

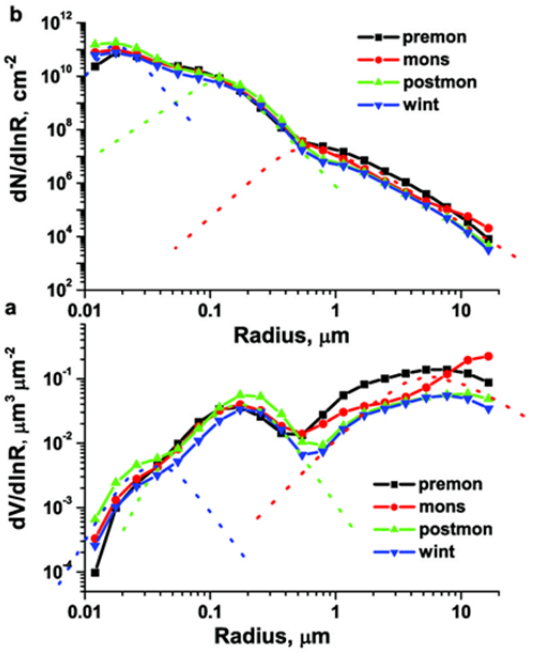

Fig. 6. a) Seasonal volume-size distribution; b) number-size distribution derived from it; three possible modes are shown with dotted lines.

Aerosol Optical Depth: Different Fractions

Variation of BC from October to May (other than monsoon period) is controlled by various types of biomass/fuel burning during festivities, generated either locally or transported by wind flow from elsewhere and day-to-day life. Apart from coagulation with other aerosol and resultant washout, temporary closing of brick kilns and absence of large scale biomass burning activities during monsoon explains the lowest observed BC in this period.

Following relations relate total AOD to absorption AOD which in turn is the sum of contributions from BC and non-BC absorbing aerosols.

$$AOD_{total} = AOD_{abs} + AOD_{scat} \;\&\; AOD_{abs} = AOD_{bc} + AOD_{non\text{-}bc\text{-}abs.} \quad (1)$$

In most of the months AOD_{bc} is less than or equal to AOD_{abs} (Fig. 7(a)) as expected. But in April and May AOD_{bc} is more than AOD_{abs} while dust particles are abundant in the air. Kim *et al.* (2004) studied properties of dust particles during ACE-Asia intensive observation period and found that there was an overestimation of coarse mode BC mass concentration by aethalometer during dusty period due to agglomeration of BC and dust particles. In addition to the possible over estimation error, scattering efficiency of coarse BC particles (mixture) could be more than fine BC particles (due to increase in size), then AAOD or AOD_{abs} (= (1 – SSA) × AOD) (Russel *et al.*, 2010) could be less than AOD_{bc} which assumes all BC aerosols are with $r_{mod}N$ equal to 0.0118 μm (Hess *et al.*, 1998) as per OPAC. This may be the reason of lower AOD_{abs} in the above months. Scarnato *et al.* (2012) studied internal mixing of BC with NaCl and found that BC internally mixed with NaCl has better SSA than BC alone and increases with more embedding common salt. Having an influx of NaCl with the onward wind from sea during this period there exists a higher possibility of BC getting embedded on NaCl, explaining the lower AOD_{abs} in July by the effective increase in SSA. AOD_{bc} is 13.4% of total AOD in March and 4.7% in June; annual average, 8.8% that is less than 11% calculated for IGB (Ramanthan and Ramana, 2005).

Aerosol Chemical Composition from OPAC

OPAC is used in this study to determine possible chemical composition based on air mass source regions through back trajectories at surface, 1500 m and 3000 m altitudes (Figs. 2(a), (b) and (c)) as well as earlier reports from the nearby regions through in-situ observations (pl. refer methodology section for settings of OPAC). The main constituents are water soluble, insoluble, soot, sea salt (acc.), and mineral accumulation/coarse and mineral transported above mixed layer. Fig. 7(b) shows monthly variation of AOD and SSA derived from OPAC and skyradiometer, is in agreement within 2% @ 500 nm.

Since AOD is mainly determined by aerosol volume, volume mixing ratios of different components are shown in Fig. 7(c). Soot, water-soluble and insoluble (Table 2) are the common components for all months but the 2 variable components are set as explained in the methodology section,

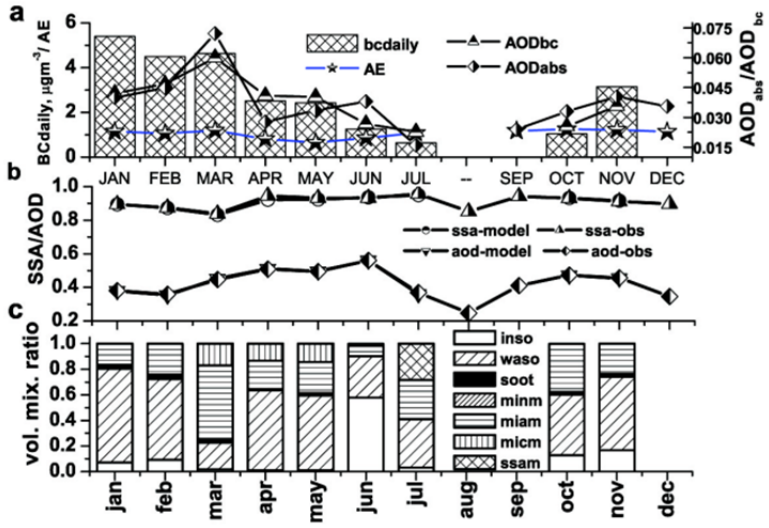

Fig. 7. a) Average day-BC concentration on monthly scale and a comparison of OPAC derived AOD_{bc} and calculated AOD_{abs} [(1 – SSA) × AOD]; b) Monthly plot of AOD and SSA (measured) vs. AOD and SSA (OPAC-derived); c) Volume mixing ratio of the different components.

but the same combination is maintained for each season. Thus mineral coarse mode is inducted during pre-monsoon and sea salt during monsoon. Transition months March (winter to pre-monsoon) and June (pre-monsoon to monsoon) have both characteristics; mineral accumulation and coarse for March (cold turning to dusty) and mineral coarse and sea salt for June (dusty turning to monsoon rain), makes it difficult to make correct prescription of components. Volume mixing ratio plot (Fig. 7(c)) portraits June with a high content of insoluble component as this also includes coarse mineral dust and in March it is the high mineral accumulation compensating some of mineral coarse mode. Sea salt accumulation mode particles are significantly high in July when air mass flows from the southern Bay of Bengal as indicated by back trajectories (Figs. 2(b) and 2(c)). Post-monsoon months October and November are associated with low winds (with short trajectories at the surface); hence aerosols are likely to have local origin. Winter and post-monsoon have similar components and also have transport of minerals at higher level. The main difference between post- monsoon and winter is the humidity related growth of aerosols and lower fog scavenging at the surface in post-monsoon. Though through OPAC it is possible to get a fair idea of chemical nature of the components; its limitations such as limited components input, only 5 types at a time that may not be the reality, are to be kept in mind. Moreover, OPAC is highly sensitive to higher humidity and insensitive from 0–50%. Similarly mixing height is also crucial in deciding AOD. OPAC is generally set for underestimation of SSA, e.g., 0.82 for urban aerosols (Hess *et al.*, 1988) that may be quite a low value looking at derived SSA from the in-situ observations (e.g., Srivastava *et al.*, 2012). However, OPAC with all its limitations remains a handy tool for many aerosol researchers.

Particulate Matter Fractions

Study location being a varied mining region it is appropriate to know the possible chemical composition and health hazard each PM bins can have. A recent study by Perrone *et al.* (2010) reports about PM_1 having sulphate enriched with Al, Ar, Cu, Cr and Zn that can reduce cell viability to half in summer which is possible at this station as well. A study in China (Tao *et al.*, 2012), with similar environment, for source apportionment of PM_1 showed secondary aerosol formation and biomass burning, diesel emissions, gasoline emissions and sea salt, and coal combustion were the greatest contributors to PM_1 in that order. Since the order of the PM_1 (derived from number concentration) is highest and cumulative number difference between $PM_{2.5}$ and PM_{10} are orders low, PM_1 concentration and relative differences of $PM_{2.5}$, PM_{10} and TSP from PM_1 are plotted in Fig. 8(a). Aerosols above PM_{10} are very low in winter as well as post monsoon and maximum sub-micron aerosols (PM_1) are in post-monsoon followed by monsoon. The significant reduction in $PM_{2.5}$ to PM_{10} in monsoon apparently points at the most effective rain-wash-out in this size-range (Croft *et al.*, 2009). Further, monsoon indicates an excess of aerosols above PM_{10}. This probably is an artifact due to increase in humidity and this part of volume-size distribution is suspected as discussed earlier. As seen in Fig. 8, a clear low in PM_1 and subsequent increase in higher sizes in pre-monsoon is associated with coarse mode aerosols transported during this period.

Since mass concentration is one of the outputs of OPAC, we have analyzed it using the respective component radii (Table 2) for quantifying pollution in the most common way (Fig. 8(b)). The station indicates poor air quality standard with $PM_{2.5}$ and PM_{10} concentrations about 10 times higher than the guideline values set by WHO viz., 10 and 20 $\mu g/m^3$ respectively. The results show that though optically pre-monsoon is the most polluted (highest AOD) and winter in terms of atmospheric heating (lowest SSA) and low dispersion (lowest mixed layer height), post-monsoon has maximum number of TSP at this station. Due to variation

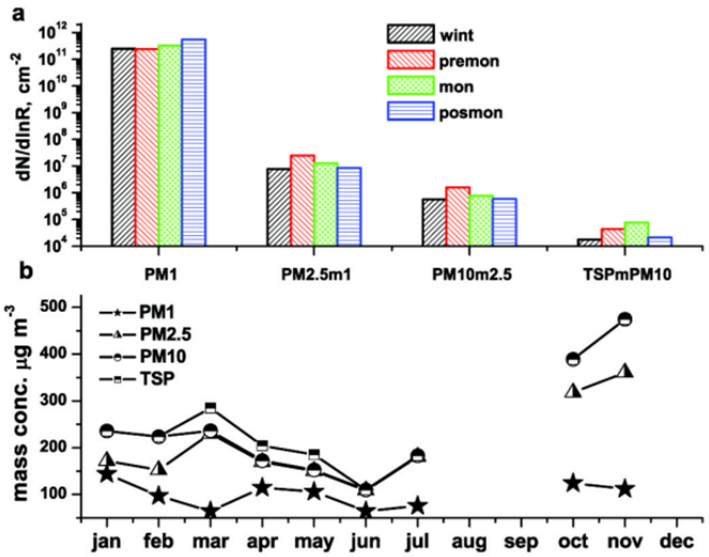

Fig. 8. a) number-size distribution of PM_1 (cumulative observed values, ref: Fig. 6(b) and difference in number from PM_1 to $PM_{2.5}$, PM_{10} and TSP; b) Monthly mass concentration in different PM size bins derived from OPAC considering modal radii.

in density, mass concentration does not follow the number concentration (Figs. 8(a) and 8(b)) but agrees with total suspended particulate matter. Chakraborty and Gupta (2010) studied PM_1 at Kanpur in 2008 and found that the concentrations are 200 (December–January), 145 (April–May), 75 (July–August) and 70 (September–October) µg/m^3. Our PM_1 values are consistent with the above results. At Delhi in 2008 the $PM_{2.5}$ measures are 100–700 (January–March), 50–75 (April–June), 50–70 (July–September) and 100–600 (October–November) µg/m^3 as reported by Tiwari *et al.* (2012). The steady increase of $PM_{2.5}$ from the start of October to November at Delhi is remarkable which is similar to the OPAC output in this study. In winter, at Ranchi $PM_{2.5}$ are much less than in Delhi but in pre-monsoon it is more as Delhi has more coarse aerosols in pre-monsoon.

CONCLUSIONS

Aerosol optical properties and chemical composition over Ranchi are summarized as follows.

1. AOD is the highest in Pre-monsoon, followed by post-monsoon and lowest in winter while SSA is the lowest in winter. Annual mean AOD and SSA are 0.43 and 0.91 respectively.
2. Angstrom exponent falls between 1 and 2 indicating intermediate size aerosols and its linear increase with AOD in winter suggests dominance of fine particles (< 1 µm).
3. OPAC derived aerosol chemical composition indicates significant volume concentration of sea salt accumulation in July, an active monsoon period, due to transport of marine aerosols as indicated by air mass back trajectories that originate in the Bay of Bengal.
4. Pre-monsoon is associated with considerable amount of mineral coarse particles that can be attributed to transport of mineral dust from IGB as well as northeast regions as corroborated by back trajectories.
5. OPAC derived AOD, SSA and fine mode radius (corresponding to the first peak in volume-size distribution) agree well with that measured by skyradiometer indicating the accuracy of aerosol chemical composition. However, in-situ measurements of chemical composition and internal/external mixing state are required for detailed understanding of aerosol properties over this complex mining plateau region as this could also affect pollution in the adjacent plains through valley flows.

ACKNOWLEDGEMENT

Analyses and visualizations used in this [study/paper/presentation] were produced with the Giovanni online data system, developed and maintained by the NASA GES DISC. The authors gratefully acknowledge the NOAA Air Resources Laboratory (ARL) for the provision of the HYSPLIT transport and dispersion model and/or READY website (http://ready.arl.noaa.gov) used in this publication. Prof. B.N. Goswami, Director, IITM is thankfully acknowledged for his support in encouraging the collaborative work with BIT, Ranchi. We thank Dipu, IITM for helping in initial installation of software.

REFERENCES

Acker, J.G. and Leptoukh, G. (2007). Online Analysis Enhances Use of NASA Earth Science Data. *Eos, Trans. Am. Geophys. Union* 88: 14–17.

Aoki, K. and Fujiyoshi, Y. (2003). Sky Radiometer Measurements of Aerosol Optical Properties over Sapporo, Japan. *J. Meteorol. Soc. Jpn.* 81: 493–513.

Babu, S.S. and Moorthy, K.K. (2001). Anthropogenic Impact on Aerosol Black Carbon Mass Concentration at a Tropical Coastal Station: A Case Study. *Curr. Sci.* 81: 208–1214.

Boi, P., Tonna, G., Dalu, G., Nakajima, T., Olivieri, B., Pompei, A., Campanelli, M. and Rao, R. (1999).

Calibration and Data Elaboration Procedure for Sky Irradiance Measurements. *Appl. Opt.* 38: 896–907.

Bréon, F., Tanré, D. and Sylvia, G. (2002). Aerosol Effect on Cloud Droplet Size Monitored from Satellite. *Science* 295: 834–838.

Chakraborty, A. and Gupta, T. (2010). Chemical Characterization and Source Apportionment of Submicron (PM_1) Aerosol in Kanpur Region, India. *Aerosol Air Qual. Res.* 10: 433–445

Chatterjee, A., Adak, A., Singh, A. K., Srivastava, M.K., Ghosh, S.K., Tiwari, S., Devara, P.C.S. and Raha, S. (2010). Aerosol Chemistry over a High Altitude Station at Northeastern Himalayas, India. *PLoS ONE* 5: e11122.

Chatterjee, A., Ghosh, S.K., Adak, A., Singh, A.K, Devara, P.C.S. and Raha, S. (2012). Effect of Dust and Anthropogenic Aerosols on Columnar Aerosol Optical Properties over Darjeeling (2200 m asl), Eastern Himalayas, India. *PLoS ONE.* 7: e40286.

Croft, B., Lohmann, U., Martin, R., Stier, P., Wurzler, S., Feichter, J., Posselt, R. and Ferrachat, S. (2009). Aerosol Size-dependent Below-cloud Scavenging by Rain and Snow in the ECHAM5-HAM. *Atmos. Chem. Phys.* 9: 4653–4675

Decesari, S., Facchini, M.C., Carbone, C., Giulianelli, L., Rinaldi, M., Finessi, E., Fuzzi, S., Marinoni, A., Cristofanelli, P., Duchi, R., Bonasoni, P., Vuillermoz, E., Cozic, J., Jaffrezo, J.L. and Laj, P. (2010). Chemical Composition of PM_{10} and PM_1 at the High-altitude Himalayan Station Nepal Climate Observatory-Pyramid (NCO-P) (5079 ma.s.l.). *Atmos. Chem. Phys.* 10: 4583–4596.

Dey, S., Tripathi, S.N., Singh, R.P. and Holben, B.N. (2004). Influence of Dust Storms on the Aerosol Optical Properties over Indo-Gangetic Basin. *J. Geophys. Res.* 199: D20211, doi: 10.1029/2004JD004924.

Dockery, D.W., Pope III CA. (1994). Acute Respiratory Effects of Particulate Air Pollution. *Auun. Rev. Publ. Health* 15: 107–132.

Draxler, R.R. and Rolph, G.D. (2013). HYSPLIT (HYbrid Single-Particle Lagrangian Integrated Trajectory) Model Access via NOAA ARL READY Website (http://ready.arl.noaa.gov/HYSPLIT.php). NOAA Air Resources Laboratory, Silver Spring, MD.

Dumka, U.C., Krishna Moorthy, K., Pant, P., Hegde, P., Sagar, R. and Pandey, K. (2008). Physical and Optical Characteristics of Atmospheric Aerosols during ICARB at Manora Peak, Nainital: A Sparsely Inhabited, High-altitude Location in the Himalayas. *J. Earth Syst. Sci.* 117: 399–405

Ghose, M.K. and Majee, S.R. (2001). Air Pollution Caused by Opencast Mining and Its Abatement Measures in India. *J. Environ. Manage*. 63: 193–202.

Ghose, M.K. (2007). Generation and Quantification of Hazardous Dusts from Coal Mining in the Indian Context. *Environ. Monit. Assess.* 130: 35–45, doi: 10.1007/s10661-006-9451-y

Gogoi, M.M., Pathak, B., Krishna Moorthy, K., Bhuyan, P.K., Babu, S.S., Bhuyan, K. and Kalita, G. (2011). Multi-year Investigations of near Surface and Columnar Aerosols over Dibrugarh, Northeastern Location of India: Heterogeneity in Source Impacts. *Atmos. Environ.* 45: 1714–172

Haywood, J.M. and Ramaswamy, V. (1998). Global Sensitivity Studies of the Direct Radiative Forcing due to Anthropogenic Sulfate and Black Carbon Aerosols. *J. Geophys. Res*. 6043–6058

Hess, M., Koepke, P. and Schultz, I. (1988). Optical Properties of Aerosols and Clouds: The software Package OPAC. *Bull. Am. Meteorol. Soc.* 79: 831–844.

Kim, W.K., He, Z. and Kim, J.Y. (2004). Physicochemical Characteristics and Radiative Properties of Asian Dust Particles Observed at Kwangju, Korea, during the 2001 ACE-Asia Intensive Observation Period. *J. Geophys. Res.* 109: D19S02, doi: 0.1029/2003JD003693

Knuckles, T.L., Stapleton, P.A., Minarchick, V.C., Esch, L., McCawley, M., Hendryx, M. and Nurkiewicz, T.R. (2013). Air Pollution Particulate Matter Collected from an Appalachian Mountaintop Mining Site Induces Microvascular Dysfunction. *Microcirculation* 20: 158–169, doi: 10.1111/micc.12014.

Kumar, R., Naja, M., Satheesh, S.K., Ojha, N., Joshi, H., Sarangi, T., Pant, P., Dumka, U.C., Hegde, P. and Venkataramani, S. (2011). Influences of the Springtime Northern Indian Biomass Burning over the central Himalayas. *J. Geophys. Res.* 116: D19302, doi: 10.1029/2010JD015509.

Lee, J., Kim, J., Song, C.H., Kim, S.B., Chun, Y., Sohn, B.J. and Holben, B.N. (2010). Characteristics of Aerosol Types from AERONET Sunphotometer Measurements. *Atmos. Environ.* 44: 3110–3117.

Levoni, C., Cervino, M., Guzzi, R., Torricella, F. (1997). Atmospheric Aerosol Optical Properties: A Database of Radiative Characteristics for Different Components and Classes. *Appl. Opt.* 36: 8031–8041

Moorthy, K.K., Babu, S.S., Satheesh, S.K., Dutt, C.B.S. and Srinivasan, J. (2007). Dust Absorption over the ''Great Indian Desert'' Inferred Using Ground-based and Satellite Remote Sensing. *J. Geophys. Res.* 112: D09206, doi: 10.1029/2006JD007690.

Moorthy, K.K. and Satheesh, S.K. (2011). Black Carbon Aerosols over India. *Black Carbone-Bulletin* 3: 1–3.

Nakajima, T., Tonna, G., Rao, R., Boi, P., Kaufman, Y. and Holben, B. (1996). Use of Sky Brightness Measurements from Ground for Remote Sensing of Particulate Polydispersions. *Appl. Opt.* 35: 2672–2686.

Novakov, T. and Penner, J.E. (1993). Large Contribution of Organic Aerosols to Cloud-condensation-nuclei Concentrations. *Nature* 365: 823–826.

Perrone, M.G., Gualtieri, M., Ferrero, L., Lo Porto, C., Udisti, R., Bolzacchini, E. and Camatini, M. (2010). Seasonal Variations in Chemical Composition and *in vitro* Biological Effects of Fine PM from Milan. *Chemosphere* 78: 1368–1377

Ram, K. and Sarin, M.M. (2010). Spatio-temporal Variability in Atmospheric Abundances of EC, OC and WSOC over Northern India. *J. Aerosol Sci.* 41: 88–98.

Ramanathan, V., Crutzen, P.J. and Kiehl, J.T. (2001). Rosenfeld D. Aerosols Climate, and the Hydrological

Cycle. *Science* doi: 10.1126/science.1064034.

Ramanathan, V. and Ramana, M.V. (2005). Persistent, Widespread, and Strongly Absorbing Haze over the Himalayan Foothills and the Indo-Gangetic Plains. *Pure Appl. Geophys.* 162: 1609–1626.

Russell, P.B., Bergstrom, R.W., Shinozuka, Y., Clarke, A.D., DeCarlo, P.F., Jimenez, J.L., Livingston, J.M., Redemann, J. Dubovik, O. and Strawa, A. (2010). Absorption Angstrom Exponent in AERONET and Related Data as an Indicator of Aerosol Composition. *Atmos. Chem. Phy.* 10: 1155–1169.

Scarnato, B., Vahidinia, S.D., Richard, D.T. and Kirchstetter, T.W. (2012). Effects of Internal Mixing and Aggregate Morphology on Optical Properties of Black Carbon Using a Discrete Dipole Approximation Model. *Atmos. Chem. Phys. Discus.* 12: 26401–26434. doi: 10.5194/acpd-12-26401-2012.

Scudlark, J.R. and Church, T.M. (1988). The Atmospheric Deposition of Arsenic and Association with Acid Precipitation. *Atmos. Environ.* 22: 937–943.

Silvia, E.D. (2002). Aerosol Impacts on Visible Light Extinction in the Atmosphere of Mexico City. *Sci. Total Environ*. 287: 213–220.

Singh, R.P., Dey, S., Tripathi, S.N., Tare, V. and Holben, B.N. (2004). Variability of Aerosol Parameters over Kanpur, Northern India. *J. Geophys. Res.* 109: D23206. doi: 10.1029/2004JD004966.

Sreekanth, V., Niranjan, K. and Madhavan, B.L. (2007). Radiative Forcing of Black Carbon over Eastern India. *Geophys. Res. Lett.* 34: L17818, doi: 10.1029/2007GL 030377.

Srivastava, A.K., Tripathi, S.N., Dey Sagnik, Kanawade, V.P. and Tiwari, S. (2012). Inferring Aerosol Types over the Indo-Gangetic Basin from ground Based Sunphotometer Measurements. *Atmos. Res.* 109–110: 64–75, doi: 10.1016/j.atmosres.2012.02.010.

Stanhill, G. and Cohen, S. (2001). Global Dimming: A Review of the Evidence for a Widespread and Significant Reduction in Global Radiation with Discussion of its Probable Causes and Possible Agricultural Consequences. *Agric. For. Meteorol.* 107: 255–278.

Tang, I. (1996). Chemical and Size Effects of Hygroscopic Aerosols on Light Scattering Coefficient. *J. Geophys. Res.* 101: 19245–19250**.**

Tao, J., Shen, Z, Zhu, C., Yue, J., Cao, J., Liu, S., Zhu, L. and Zhang, R. (2012). Seasonal Variations and Chemical Characteristics of Sub-micrometer Particles (PM_1) in Guangzhou, China. *Atmos. Res.* 118: 222–231

Tiwari, S., Chate, D.M., Srivastava, A.K., Bisht, D.S. and Padmanabhamurty, B. (2012). Assessments of PM_1, $PM_{2.5}$ and PM_{10} Concentrations in Delhi at Different Mean Cycles. *Geofizika* 29: 51–67

Venkataraman, C., Habib, G., Kadamba, D., Shrivastava, M., Leon, J.F., Crouzille, B., Boucher, O. and Streets, D.G. (2006). Emissions from Open Biomass Burning in India: Integrating the Inventory Approach with High Resolution Moderate Resolution Imaging Spectro-radiometer (MODIS) Active-fire and Land Cover Data. *Global Biogeochem. Cycles* 20: GB2013, doi: 10.1029/ 2005B002547.

Wang, C., Kim, D., Ekman, A.M.L., Barth, M.C., Rasch, P.J. (2009). Impact of Anthropogenic Aerosols on Indian Summer Monsoon. *Geophys. Res. Lett.* 36: L21704, doi: 10.1029/2009GL040114.

Yang, X. and Wenig, M. (2009). Study of Columnar Aerosol Size Distribution in Hong Kong. *Atmos. Chem. Phys.* 9: 6175–6189.

Received for review, February 28, 2013
Accepted, July 8, 2013